

# The axial breathing mode in rapidly rotating Bose-Einstein condensates

Gentaro Watanabe

<sup>a</sup>*NORDITA, Blegdamsvej 17, DK-2100 Copenhagen Ø, Denmark*

<sup>b</sup>*RIKEN, 2-1 Hirosawa, Wako, Saitama 351-0198, Japan*

(Dated: May 24, 2019)

Measurements of the axial breathing mode frequency in a rotating Bose-Einstein condensate show a strong dependence on the rotation rate when this is close to the transverse trap frequency. We show that the data agree well with a calculation based on a generalized lowest Landau level wave function, in which the length in the Gaussian factor is treated as a variable. The zero point energy in the direction of the rotation axis is an essential ingredient for explaining the data.

PACS numbers: 03.75.Kk, 05.30.Jp, 67.40.Vs, 47.37.+q

The creation of vortices in atomic Bose-Einstein condensates has opened up a new horizon in the study of superfluids. This novel system enables us to investigate an unexplored regime, in which the vortex core is comparable to the intervortex distance since the interaction energy per particle  $\sim gn$  is much smaller than that of liquid helium 4 (see, e.g., Ref. [1] and references therein). Here  $n$  is the particle number density and  $g \equiv 4\pi\hbar^2 a_s/m$  is the two-body interaction strength,  $m$  is the particle mass, and  $a_s$  is the  $s$ -wave scattering length.

For a harmonically trapped Bose-Einstein condensate, when the rotation angular velocity  $\Omega$  is close to the transverse trapping frequency  $\omega_\perp$ , so that  $\hbar\Omega \gtrsim gn$ , the condensate wave function is dominated by the lowest Landau level (LLL) component [2]. When the number of particles  $N$  is much larger than the number of vortices  $N_v$ , the system may be described by the Gross-Pitaevskii equation [3, 4]. Recently, Schweikhard *et al.* [5] have reached what we shall refer to as the mean-field LLL regime [6, 7, 8, 9, 10], in which  $\hbar\Omega \gtrsim gn$  with  $N \gg N_v$ .

In Ref. [5], Schweikhard *et al.* have measured the axial breathing mode frequency and they have observed a frequency shift in the rapid rotation regime, which cannot be described by the hydrodynamic model of Ref. [11]. We have studied breathing modes in the mean-field LLL regime in Ref. [12], and have pointed out that our theoretical framework developed there could describe this frequency shift. The purpose of this Brief Report is to compare in detail our theoretical prediction of the axial breathing mode frequency with experimental data. We shall show that our calculations explain well the behavior of the experimental data.

In the Appendix of Ref. [12], in which we discussed the breathing modes in three dimensions, we employed a generalized LLL wave function  $\phi_{\text{ex}}$ , in which the transverse oscillator length is treated as a variable. There we assumed the coarse-grained density profile  $\langle|\phi_{\text{ex}}|^2\rangle$  to be a Thomas-Fermi parabola in the transverse direction and

a Gaussian form in the axial ( $z$ -) direction, i.e.,

$$\langle|\phi_{\text{ex}}|^2\rangle = \nu(0) \left(1 - \frac{r^2}{R_\perp^2}\right) e^{-z^2/\sigma_z^2}, \quad (1)$$

where  $R_\perp$  is the Thomas-Fermi radius in the transverse direction, and  $\sigma_z$  is the cloud width in the axial direction. The constant  $\nu(0) = 2\pi^{-3/2}/(R_\perp^2\sigma_z)$  is chosen so that  $\langle|\phi_{\text{ex}}|^2\rangle$  satisfies the normalization condition  $\int d^3r \langle|\phi_{\text{ex}}|^2\rangle = 1$ . The assumption of the Gaussian axial density profile would be reasonable in the rapid rotation regime, in which the cloud is so dilute that  $\hbar\omega_z \gtrsim gn$ , where  $\omega_z$  is the axial trapping frequency.

Using the variational Lagrangian formalism, we obtained coupled equations that determine  $R_\perp$  and  $\sigma_z$  in the equilibrium state [12]:

$$\left(1 - \frac{\Omega_0^2}{\omega_\perp^2}\right) X_0^4 - 8\kappa_{3D} Z_0^{-1} = 0, \quad (2)$$

and

$$Z_0^3 - Z_0^{-1} - \frac{8\kappa_{3D}}{3} \frac{\omega_\perp}{\omega_z} X_0^{-2} = 0. \quad (3)$$

Here  $X_0$  and  $Z_0$  are the equilibrium values of  $X \equiv R_\perp/d_\perp$  and  $Z \equiv \sigma_z/d_z$ , where  $d_\perp \equiv \sqrt{\hbar/m\omega_\perp}$  and  $d_z \equiv \sqrt{\hbar/m\omega_z}$  are the transverse and the axial oscillator length, respectively, and  $\Omega_0$  is the rotation velocity in the equilibrium state. The quantity

$$\kappa_{3D} \equiv \frac{mbgN}{2\pi\hbar^2} \frac{1}{\sqrt{2\pi}d_z} \quad (4)$$

is the dimensionless interaction strength, where  $b \equiv \langle|\phi_{\text{ex}}|^4\rangle/\langle|\phi_{\text{ex}}|^2\rangle^2$  is the Abrikosov parameter, which is comparable to unity.

The expression for the radial and axial breathing mode frequencies is (Eq. (A16) in Ref. [12])

$$\omega^2 = \frac{1}{2} \left[ \left(3 + \frac{1}{Z_0^4}\right) \omega_z^2 + 4\omega_\perp^2 \right] \pm \frac{1}{2} \sqrt{\left[ \left(3 + \frac{1}{Z_0^4}\right) \omega_z^2 - 4\omega_\perp^2 \right]^2 + 8\omega_\perp^2 \omega_z^2 \left(1 - \frac{\Omega_0^2}{\omega_\perp^2}\right)}. \quad (5)$$

The  $1/Z_0^4$  terms come from the zero-point energy in the  $z$ -direction, which is not taken into account in the hydrodynamic calculation [11] based on the Thomas-Fermi theory [13].

Note that Eq. (5) can describe the frequency shift of the axial breathing mode from  $\omega = \sqrt{3}\omega_z$  to  $2\omega_z$  in the fast rotation regime reported in Ref. [5]. For values of  $\Omega_0$  on which we shall focus, the second term in the square root of Eq. (5) can be neglected and this equation reduces to

$$\omega^2 \simeq 4\omega_{\perp}^2 \quad \text{and} \quad \left(3 + \frac{1}{Z_0^4}\right)\omega_z^2, \quad (6)$$

where the former result is for the transverse breathing mode and the latter is for the axial one. Since  $Z = \sigma_z/d_{\perp} \geq 1$ , the former case is given by the upper sign and the latter by the negative one for  $\omega_{\perp} > \omega_z$  (opposite for  $\omega_{\perp} < \omega_z$ ). If the system is in the LLL limit,  $z$ -dependence of the wave function corresponds to the ground state of a particle in a harmonic potential, i.e.,  $Z_0 \simeq 1$ , and thus the latter expression of Eq. (6) leads to  $\omega \simeq 2\omega_z$ . Otherwise  $1/Z_0^4$  term is small and this expression gives  $\omega \simeq \sqrt{3}\omega_z$ . This observation shows that the zero-point energy in the  $z$ -direction, which is neglected in the Thomas-Fermi theory, plays an essential role in the frequency shift of the axial breathing mode. We also note that, from the first expression of Eq. (6), such a change in the mode frequency does not exist for the radial breathing mode [14].

To compare experimental data and our theoretical calculation on the axial breathing mode frequency in the fast rotation regime, unlike Ref. [5], we do not use the Thomas-Fermi theory to evaluate the rotation velocity  $\Omega_0$ . In the experiment of Ref. [5], the Thomas-Fermi radius  $R_z$  in the  $z$ -direction has been measured for the axial extent of the cloud. Together with  $R_{\perp}$ ,  $R_z$  is determined by fitting the Thomas-Fermi density profile integrated along the  $x$ - (or  $y$ -) direction [15]. However, in our theoretical framework, the Gaussian axial density profile is assumed and thus the experimental data of  $R_z$  cannot be used for  $Z_0$  directly. For the above reasons, we treat  $\Omega_0$  and  $Z_0$  as unknown variables in analyzing the experimental data. In the following analysis, we use the same values of the experimental parameters as those in Ref. [5], i.e.,  $\omega_{\perp} = 2\pi \times 8.3$  Hz ( $d_{\perp} \simeq 3.7$   $\mu\text{m}$ ),  $\omega_z = 2\pi \times 5.3$  Hz ( $d_z \simeq 4.7$   $\mu\text{m}$ ), and  $a_s \simeq 5.6$  nm. For the Abrikosov parameter, we use the value in the LLL limit for a regular triangular lattice,  $b = 1.1596$ , but the results do not change significantly even for the value  $b = 1$  for the small vortex core limit.

Using the coupled equations (2) and (3), we can determine  $\Omega_0$  and  $Z_0$  for each shot of the experiment from the measured values of  $R_{\perp}$  and  $N$  [15]. In Fig. 1, we plot the number of particles with respect to  $\Omega_0$  (note that these values of  $\Omega_0$  are different from the rotation velocity determined by the Thomas-Fermi theory shown in Fig. 2 of Ref. [5]). We model the experimental data by fitting

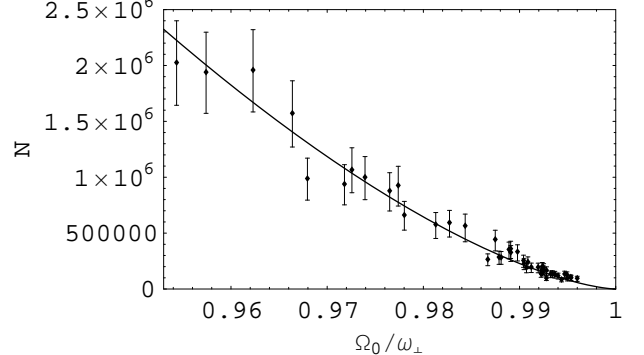


FIG. 1:  $\Omega_0$  dependence of the number of particles  $N$ . The points with error bars show experimental data provided by Schweikhard [15]. The solid line shows a function  $N(\Omega_0)$  used in the theoretical calculation, which is determined by fitting the data with a form of  $c(1 - \Omega_0/\omega_{\perp})^{3/2}$ .

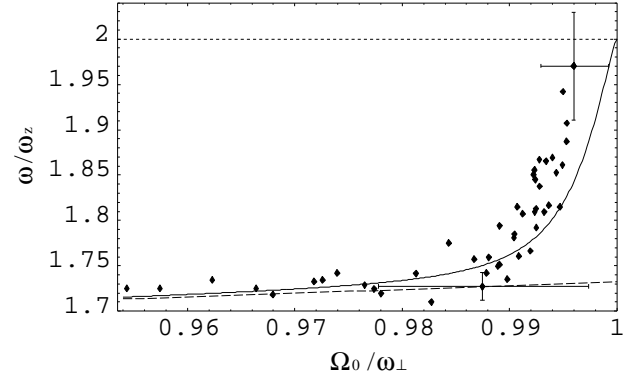


FIG. 2: Axial breathing mode frequency  $\omega$  as a function of  $\Omega_0$ . The points are the experimental data and the solid line shows our theoretical result. The dashed line shows the result of a hydrodynamic model by Ref. [11].

them with a function of the following form:

$$N(\Omega_0) = c \left(1 - \frac{\Omega_0}{\omega_{\perp}}\right)^{3/2}, \quad (7)$$

with  $c = 2.281 \times 10^8$ .

With  $N(\Omega_0)$  given by Eq. (7),  $X_0$  and  $Z_0$  for a given value of  $\Omega_0$  are determined by the coupled equations (2) and (3). Then we can calculate from Eq. (5) the axial breathing mode frequency for each  $\Omega_0$ . In Fig. 2, we plot the resulting axial breathing mode frequency  $\omega$  as a function of  $\Omega_0$ , and compare it with the experimental data. The errors in  $\Omega_0$  are estimated from the errors in  $N$  and  $R_{\perp}$  [15] by use of the error propagation law and the errors in  $\omega$  are the same as those in Fig. 2 of Ref. [5]. We note that, unlike the previous Thomas-Fermi calculation (the dashed line in Fig. 2), our theoretical curve reproduces the behavior of the experimental data within the scatter of the data points and the error bars.

We see that the error in  $\Omega_0$  for the data point with

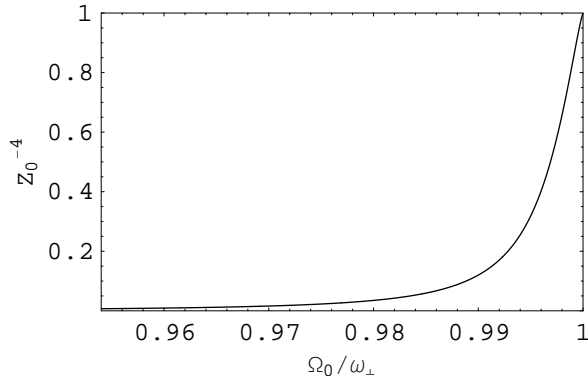


FIG. 3: Contribution  $Z_0^{-4}$  of the zero-point energy of the  $z$ -direction to the axial breathing mode frequency as a function of  $\Omega_0$ .

lower  $\Omega_0$  is fairly larger than the error for the other data point in this figure and that in Fig. 2 of Ref. [5]. The reason is that, in the present analysis, we use measured  $N$  to determine  $\Omega_0$  of each experimental shot unlike Ref. [5] in which the rotation velocity is determined only by the aspect ratio of the cloud, and an error in  $N$  for this data point is about four times larger than that of the other one.

In Fig. 3, we plot  $Z_0^{-4}$ , which is the contribution of the zero-point energy of the  $z$ -direction to the axial breathing mode frequency. We see that this quantity increases rapidly between  $\Omega_0/\omega_{\perp} \gtrsim 0.99$  and  $\Omega_0/\omega_{\perp} = 1$ , which directly reflects in the behavior of  $\omega$  shown in Fig. 2. As has been discussed in Ref. [12], the sudden increase of  $Z_0^{-4}$  and the frequency shift of the axial breathing mode occurs when the interaction energy per particle falls below  $\hbar\omega_z$  and we actually confirm that the ratio  $\hbar\omega_z/gn \sim (R_{\perp}^2/d_z^2)(Na_s/Z)^{-1}$  is comparable to unity at  $\Omega_0 \simeq 0.99\omega_{\perp}$ .

As can be seen from Fig. 2, our calculations can account semi quantitatively for the rise of the axial breathing mode frequency. However, the agreement is not perfect, and we now discuss possible reasons for this. In the present analysis, the value of  $\Omega_0$  for a particular data point depends on the measured value of  $N$ , which is difficult to determine accurately in the fast rotation regime. Another possible source of error is that the rotation axis may not be exactly perpendicular to the imaging beam, but is tilted up to 5 degrees [15]. This inclination leads to an overestimate of  $R_z$  and consequently of  $N$ . This effect is serious in the fast rotation regime in which the cloud is very flat, but it has not been taken into account explicitly in the values of  $N$  deduced from experiment because the tilt angle cannot be measured in the experiment. (However the error bars on  $N$  include a contribution due to the uncertainty in the inclination angle.) An overestimate of  $N$  leads to smaller  $\Omega_0$  for the experimental data points shown in Fig. 2.

In this work, we have analyzed the axial breathing mode frequency in the fast rotation regime using our theoretical framework developed in Ref. [12]. We have compared the theoretical calculation with the experimental results obtained by Schweikhard *et al.* [5, 15] in detail and have shown that they agree within the scatter of the data points and the error bars. The contribution of the zero-point energy in the  $z$ -direction is an essential ingredient for the change of the mode frequency from  $\sqrt{3}\omega_z$  to  $2\omega_z$ . Our framework have achieved a significant improvement over the previous calculations [11, 16] in explaining the breathing mode in the rapid rotation regime.

The author is very grateful to Volker Schweikhard for generously providing us with his experimental data, and for many valuable comments. He also thanks Chris Pethick for helpful discussion and comments. This work was supported by the JSPS Postdoctoral Fellowship for Research Abroad.

---

[1] I. Coddington *et al.*, Phys. Rev. A **70**, 063607 (2004).  
[2] T.-L. Ho, Phys. Rev. Lett. **87**, 060403 (2001).  
[3] N. R. Cooper, N. K. Wilkin, and J. M. F. Gunn, Phys. Rev. Lett. **87**, 120405 (2001).  
[4] J. Sinova, C. B. Hanna, and A. H. MacDonald, Phys. Rev. Lett. **89**, 030403 (2002).  
[5] V. Schweikhard *et al.*, Phys. Rev. Lett. **92**, 040404 (2004).  
[6] G. Watanabe, G. Baym, and C. J. Pethick, Phys. Rev. Lett. **93**, 190401 (2004).  
[7] N. R. Cooper, S. Komineas, and N. Read, Phys. Rev. A **70**, 033604 (2004).  
[8] A. Aftalion, X. Blanc, and J. Dalibard, Phys. Rev. A **71**, 023611 (2005).  
[9] E. B. Sonin, Phys. Rev. A **72**, 021606(R) (2005).  
[10] M. Cozzini, S. Stringari, and C. Tozzo, cond-mat/0509559.  
[11] M. Cozzini and S. Stringari, Phys. Rev. A **67**, 041602(R) (2003).  
[12] G. Watanabe, to appear in Phys. Rev. A (cond-mat/0506331).  
[13] With neglect of the  $1/Z_0^4$  terms, Eq. (5) reduces to Eq. (10) in Ref. [11] derived within the Thomas-Fermi theory. This means that Eq. (5) is valid also in the slow rotation regime even though this expression is derived assuming the system is in the mean-field LLL regime. The reason for this validity is explained in the Appendix of Ref. [12].  
[14] There is, of course, a small change in the radial breathing mode frequency  $\omega_{\text{rad}}$  due to the neglected  $1 - (\Omega_0^2/\omega_{\perp}^2)$  term of Eq. (5). For  $\omega_{\perp} > \omega_z$ ,  $\omega_{\text{rad}}$  is given by the upper (positive) sign and thus  $\omega_{\text{rad}}$  decreases to  $2\omega_{\perp}$  with increasing  $\Omega_0$  (for  $\omega_{\perp} < \omega_z$ ,  $\omega_{\text{rad}}$  increases to  $2\omega_{\perp}$  with increasing  $\Omega_0$ ). However, this change is quite small in the all cases considered in this paper.  
[15] V. Schweikhard, private communication.  
[16] S. Choi, L. O. Baksmaty, S. J. Woo, and N. P. Bigelow, Phys. Rev. A **68**, 031605(R) (2003).